2021

A Gray-Box Dynamic Modeling Method for Variable Speed Direct Expansion Systems

Haopeng Liu
University of Oklahoma, United States of America, jcai@ou.edu

Jie Cai

A gray-box dynamic modeling method for variable speed direct-expansion systems

Haopeng Liu[1], Jie Cai[1]

[1]School of Aerospace and Mechanical Engineering, University of Oklahoma, Norman, OK, US
Haopeng.Liu-1@ou.edu, jcai@ou.edu

ABSTRACT

In this paper, a gray-box dynamic modeling approach for variable-speed direct-expansion systems is presented. The overall approach incorporates a multi-stage training procedure that consists of 1) identification of component sub-models from quasi-steady-state performance data, 2) system model integration with estimation of refrigerant charge and 3) fine tuning of thermal capacitances of the evaporator and condenser to capture the system dynamic responses. Compared to traditional physics-based models, the proposed modeling approach has advantages including reduced engineering efforts in the model development phase, improved computational efficiency and reduced uncertainties. The modeling method was applied to a 3-ton variable-speed heat pump and proved to be capable of accurately capturing the system transient behaviors over a wide range of operating conditions.

1. INTRODUCTION

Vapor compression cycles are predominantly used for air conditioning and refrigeration systems. According to EIA reports (2020), buildings account for nearly 70% of electricity use and more than 35% of the building electrical energy consumption is associated with vapor compressor cycle-based equipment. Therefore, reliable models of vapor compression systems (VCS) with moderate computational requirements is crucial to achieve maximum energy performance through optimized system design and control synthesis.

A good number of papers can be found in the literature on steady-state modeling of VCS. For example, Navarro *et al*. (2010) presented a steady-state model of variable speed VCS for predicting system coefficients of performance (COP) under variable compressor speed and boundary conditions. The single phase regions (e.g. superheat phase) were not considered during the modeling of heat exchangers, which may deteriorate the accuracy of the proposed model. In contrast, Belman *et al*. (2006) proposed a new model form that considers superheat temperature as an influential input and models the different fluid regions (two phase and single phase) separately, in order to improve the prediction accuracy. Although steady-state models are useful for system performance evaluation and design, they are not directly usable for control system design, which is a challenging task for variable-speed VCS.

Dynamic models of direct-expansion (DX) systems, on the other hand, capture system transient behaviors and thus, are suitable for system dynamic analysis and controller design. Given that the thermal dynamics associated with the heat transfer processes in evaporators and condensers are dominant in the overall system transience, the primary focus of relevant efforts was on dynamic performance characterization of heat exchangers. Furthermore, previous survey studies (Bendapudi and Braun, 2002, Rasmussen, 2012) indicated that most of the research interests were focused on capturing two phase flow dynamics of heat exchangers which to a large extent determine the evolution of system pressures. Since the dynamics of compressors and expansion valves are much faster, their transient behaviors are usually not considered and quasi-steady-state models are adopted for development of dynamic DX system models. Catano *et al*. (2013) proposed a lumped-parameter dynamic model of DX systems to facilitate development of gain scheduling control. The heat exchangers were assumed to be two phase and quasi-steady-state models were adopted for the compressor and electronic expansion valve (EXV). The resulting model is computationally efficient with only a few governing equations and model parameters. However, the lumped approach can't provide accurate predictions of system performance (e.g. cooling capacity, refrigerant charge) due to the averaging effect of state variables, e.g. refrigerant density and enthalpy. In contrast to the lumped method that models the whole heat exchanger with a single control volume, the moving boundary (MB) method seeks to capture the major dynamics of multi-phase heat exchangers while preserving the simplicity of the lumped approach. Chen and Deng (2006) developed a dynamic

model of variable air volume (VAV) DX systems for control analysis, where the MB approach with empirical heat transfer correlations was applied for modeling of heat exchangers. The nonlinear dynamic features such as hysteresis and dead band were also all taken into consideration. The major drawback of the MB method lies on the numerical instability when a single phase region disappears or reappears; to this end, an improved version of the MB approach, termed switched MB (SMB), was proposed and various switching strategies were studied. For instance, Li and Alleyne (2010) presented a SMB method for DX systems, to facilitate analysis of the transient behaviors of heat exchangers during system shut-down and start-up. The normalized length of the single-phase region was compared to a pre-determined threshold to switch between the two-region and one-region model forms for the evaporator. A natural extension of the MB approach, i.e., the finite control volume method, considers multiple control volumes to capture system responses at a higher granularity. Kapadia *et al*. (2009) presented a finite control volume model of DX air conditioning system to predict system transient characteristics (refrigerant pressure) during start-up. Beghi and Cecchinato (2010) used a similar finite control volume model to assist design of an auto-tuned PID controller for EXV, where constraints imposed by the actuation system such as upper bound and hysteresis were accounted for explicitly. The delay in system response was handled via Pade-approximation so that linear system theory could be applied.

The modeling methods described above would require geometric details of the heat exchangers, the acquisition of which could be time consuming. Pure data-driven models require large training data set to achieve satisfactory extrapolating performance and acquisition of the training data could be cost prohibitive for engineering practices. To address the above challenges, a reliable gray-box dynamic modeling method for variable-speed DX systems is presented in this paper. Employing a finite control volume approach, the established model can capture the system dynamics with adequate accuracy. Training of the model is carried out in multiple stages: 1) the key parameters (e.g. heat transfer correlations) for the component models are estimated separately based on steady-state performance data to reduce computational requirements; 2) a system model is then established by integrating the component models together through continuity equations where the total refrigerant charge is estimated; 3) the steady-state system model is finally transformed into a dynamic system model through state-space governing equations, where the heat exchanger thermal capacitances are estimated from transient operation data. The proposed method has advantages including low training data requirement and high computational efficiency. Experimental validation was conducted for a 3-ton variable-speed heat pump to demonstrate the effectiveness of our methodology.

2. METHODOLGY

The overall modeling methodology consists of a hierarchical training procedure as shown in Figure 1. The bottom layer involves identification of steady-state component models associated with the heat exchangers, compressor and EXV. In the middle layer, the established component models are integrated through continuity equations to obtain a system model in which the charge level is estimated by matching the predicted steady-state cooling capacity and the measurements. The top layer transforms the steady-state model into a dynamic one described by state-space governing equations and the optimal wall thermal capacitances of the heat exchangers are identified to best reproduce the system transient responses. The bottom and middle layers are designed to identify the steady-state models and these processes consume minimum computational resources. The top layer implements iterations of dynamic simulations for parameter estimation, which is a computationally demanding task; however, it only involves two estimation parameters, resulting in much reduced iterations. This hierarchical training methodology is able to establish a data-driven dynamic model for VCS in a very efficient manner. More importantly, decoupled estimation of the various groups of model parameters reduces the risk of potential over-parameterization issues and generates a more reliable model with minimum correlations between parameters.

The following assumptions are made for modeling of the system

- Refrigerant-side pressure drops are neglected for both the evaporator and condenser.
- Counter-flow heat transfer is assumed for both heat exchangers.
- The EXV model is not explicitly used when estimating the refrigerant charge; instead, the superheat is assumed to always match the measured value, which is represented by an equality constraint in the steady-state model integration step (middle layer).
- Dynamics for the air-side of the heat exchangers, compressor and EXV are neglected.

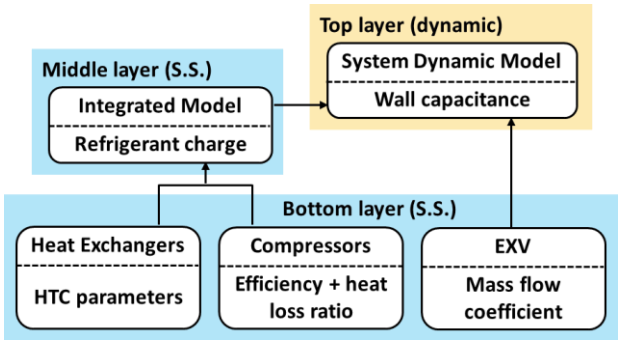

Figure 1: Overall schematic diagram of methodology

This section firstly describes the steady-state component models that can be estimated separately (bottom layer). Then they are integrated through continuity constraints to establish a complete steady-state system model (middle layer). Lastly, training of the dynamic system model is presented, in which only two estimation parameters, i.e., thermal capacitances of heat exchanger tube walls, are involved.

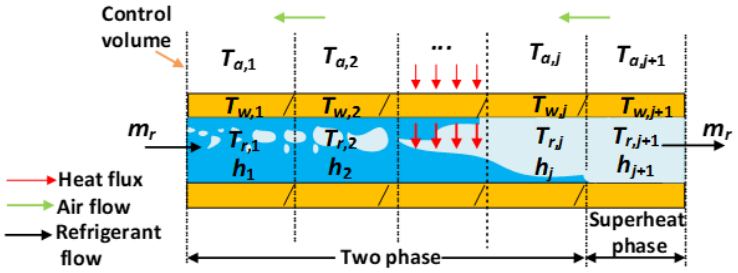

Figure 2: Schematic diagram for the finite control volume model of the evaporator

2.1 Steady-state model identification

Gray box models for the various components of a DX system are firstly presented. The component models capture the respective physics through heat and mass balances together with empirical correlations whose parameters are estimated based on experimental test data. The identified component models are then integrated into a system model to estimate the refrigerant charge level. Both the component and system models presented in this section capture the steady-state behaviors.

2.1.1 Evaporator

A finite control volume approach is adopted for modeling of the evaporator. A schematic diagram is given in Figure 2. This method divides a heat exchanger into multiple control volumes and analyzes the heat exchange characteristics of each control volume according to the local refrigerant thermal status. For the j^{th} control volume, the following energy balance equation characterizes the heat exchange between the air and refrigerant:

$$q_j = \alpha_{r,j} A_{i,j} \left(T_{w,j} - T_{r,j}\right) = \alpha_{a,j} A_{o,j} \left(T_{a,j} - T_{w,j}\right) = m_r \left(h_j - h_{j-1}\right) = C_{p,a} m_a \left(T_{a,j+1} - T_{a,j}\right) \quad (1)$$

where q_j is the heat transfer rate, $\alpha_{r,j}$ and $\alpha_{a,j}$ represent the refrigerant- and air-side HTCs, respectively, $A_{i,j}$ and $A_{o,j}$ denote the inner and outer heat transfer areas of the tube, respectively. $T_{w,j}$, $T_{r,j}$ and $T_{a,j}$ are the tube wall, refrigerant and air temperatures, respectively. $T_{a,j+1}$ and $T_{a,j}$ are the air inlet and outlet temperatures. m_r and m_a are the mass flow rates of the refrigerant and airflow, $C_{p,a}$ is the air specific heat and h_j is the enthalpy of the j^{th} control volume. The refrigerant enthalpy is assumed to be uniform across each control volume. Therefore, h_j can also be regarded as the outlet enthalpy of the j^{th} control volume.

The main unknowns in Equation (1) are the refrigerant- and air-side HTCs. The gray box component models are to estimate the HTCs based on local operating conditions and the thermal properties. The simplified exponential form derived from Wang *et al*. (1997) correlation is used to estimate the air side HTC $\alpha_{a,e}$ from mass flow rate m_a

$$\alpha_{a,e}A_{o,e} = a_1 m_a^{a_2} \tag{2}$$

where the subscript *e* stands for evaporator, a_1 and a_2 are parameters that need to be estimated in the training process.

For estimation of the refrigerant side evaporation HTC, a simplified form based on the Chen (1966) correlation is proposed as shown in Equation (3)

$$\alpha_{tp,e} = \theta_1 T_e^{\theta_2} \Delta T_{sat}^{\theta_3} \left(\frac{1}{1+\theta_4 Re_{tp}^{\theta_5}} \right) + \theta_6 \chi_{tt}^{\theta_7} \alpha_{l,e} \tag{3}$$

where θ_1 to θ_7 are parameters to be estimated in the training procedure, T_e is the saturated evaporating temperature, ΔT_{sat} is the temperature difference between of the tube wall (T_{wall}) and T_e, Re_{tp} is the two phase Reynolds number. $\alpha_{l,e}$ is the liquid phase convective HTC obtained using the turbulent flow correlation of Dittus-Boelter (Bergman *et al*., 2011). χ_{tt} is the Martinelli parameter which is a function of refrigerant quality *q*.

The two phase heat transfer dominates the total cooling effect of the evaporator while the superheat region only accounts for a small fraction of the heat exchange. Therefore, to improve model identifiability, the gray-box model adopts the Gnielinski correlation (Admiraal *et al*., 1993) for the superheated phase directly, without any training.

The refrigerant inventory strongly affects the overall system behavior. Estimation of the refrigerant mass inside heat exchangers often relies on void fraction correlations for two-phase flow. Assuming the heat flux is constant and no liquid is entrained in the central vapor core, this study utilizes the void fraction correlation given in Tandon et al. (1985) to estimate the refrigerant charge.

2.1.2 Condenser

The air-side HTC of the condenser can be estimated using a similar correlation proposed for the evaporator. However, the test unit has a fixed condenser fan speed and therefore, the air-side HTC $\alpha_{a,c}$ is a constant parameter that can be estimated in the training process.

For estimation of the refrigerant side HTC $\alpha_{tp,c}$, the following simplified form that closely resembles the Shah correlation (Shah, 1979) is used

$$\alpha_{tp,c} = \alpha_{l,c} \left[c_1 (1-q)^{c_2} + c_3 q^{c_4} T_c^{c_5} \right] \tag{4}$$

where c_1 to c_5 are parameters to be estimated in the training procedure, T_c is the saturated condensing temperature, $\alpha_{l,c}$ is the liquid phase convective HTC. It is noteworthy that when the quality *q* approaches zero in Equation (4) the condensation HTC converges to $\alpha_{l,c}$. Therefore Equation (4) guarantees a smooth transition of the HTC at the interface between the two-phase and subcooled regions and can capture the heat transfer characteristics for these two regions. Similar to the evaporator case, the gray-box model assumes the Gnielinski correlation (Admiraal *et al*., 1993) for the desuperheated region and no training is involved. Besides, the void fraction of condenser assumes the same correlation for the evaporator.

2.1.3 Compressor

As mentioned in the previous sections, a quasi-steady-state model is used to model the compressor characteristics considering its fast dynamics relative to those of the evaporator and condenser. The refrigerant mass flow rate m_r pumped by a scroll compressor is calculated as (Winandy et al., 2002)

$$m_r = \frac{V_s \cdot RPM}{60 \upsilon_{suc}} \tag{5}$$

where υ_{suc} is the specific volume of refrigerant at the suction port, *RPM* denotes the compressor speed, V_s represents the swept volume of the compressor, which is the only estimation parameter for the refrigerant mass flow sub-model.

The electrical power input to the compressor is modeled based on estimating the work necessary for a polytropic compression process corrected by a combined isentropic efficiency and a heat loss ratio associated with the heat exchange between the compressor shell and the environment. Equation (6) shows the power calculation model (Reindl et al., 2000):

$$Power \cdot (1 - f_{hl})\eta_{comb} = m_r (h_{dis} - h_{suc})\eta_{comb} = m_r \underbrace{\left\{ \frac{\lambda}{\lambda - 1} P_e \upsilon_{suc} \left[(P_c / P_e)^{\frac{\lambda - 1}{\lambda}} - 1 \right] \right\}}_{\text{ideal isentropic enthalpy gain}} \tag{6}$$

where η_{comb} is the combined isentropic efficiency, f_{hl} is the heat loss ratio, h_{dis} and h_{suc} are discharge and suction enthalpy, respectively, λ is the specific heat ratio, P_c and P_e denote condensing and evaporating pressures, respectively. The term of the right-hand side inside the curly brackets gives the refrigerant enthalpy gain for ideal compression. Chen (*et al*., 2000) has shown that the isentropic efficiency has strong dependence on the pressure ratio P_c/P_e and *RPM*. The polynomial correlation given in Equation (7) is proposed for estimation of the combined efficiency, based on the experimental data collected in the present study. A linear correlation is used for predicting the heat loss ratio f_{hl} for given compressor speed and ambient temperature, as shown in Equation (8).

$$\eta_{comb} = d_1 + d_2 \mathrm{In}(P_c / P_e) + d_3 RPM + d_4 \mathrm{In}(P_c / P_e) \cdot RPM \tag{7}$$

$$f_{hl} = e_1 + e_2 RPM + e_3 T_s \tag{8}$$

where d_1 to d_4 and e_1 to e_3 are estimation parameters, and T_s is the outdoor air temperature.

2.1.4 EXV

EXV is increasingly used in modern VCS because of its fast and accurate response to superheat changes as well as robust adaptability to time varying operation conditions. The refrigerant flow through the EXV is calculated with (Li, 2013)

$$m_r = C_d A Y \sqrt{2\rho_f (P_c - P_e)} \tag{9}$$

where *A* is the throat area of the EXV when it's fully open, ρ_f is the saturated liquid phase refrigerant density on the condenser side. *Y* is the expansion factor accounting for the increase of refrigerant specific volume, which is only used when two-phase refrigerant enters the EXV and is dependent on the pressure ratio and thermal properties (e.g. specific heat) of refrigerant (Davies and TC, 1973). When sub-cooled refrigerant enters the EXV (i.e., subcooling is nonzero), the expansion factor assumes unity. The mass flow coefficient C_d is a dimensionless variable that varies with the valve opening *z* and subcooling T_{sb}. The following polynomial was found appropriate to capture the EXV behavior from the experimental data:

$$C_d = f_1 + f_2 z + f_3 z^2 + f_4 z (T_{sub} / T_c) \tag{10}$$

where T_c is the critical temperature of the refrigerant, and f_1 to f_4 are estimation parameters.

The component models described in sections 2.1.1 to 2.1.4 can be trained separately using quasi-steady-state performance data. A robust training methodology proposed by the authors (Liu and Cai, 2021), which includes sensitivity analysis and de-correlating steps to avoid over-parameterization issues, is used in estimating the steady-state component models. The training process aims to identify the optimal parameter values to minimize the root mean square relative error (RMSRE) between the predicted output and experimental data:

$$\text{RMSRE} = \sqrt{\frac{1}{K}\sum_{i=1}^{K}\left(\frac{y_{mea}^{i} - y_{est}^{i}}{y_{mea}^{i}}\right)^{2}} \times 100\% \tag{11}$$

where K represents the number of data points, y_{mea}^{i} and y_{est}^{i} are the measured and the predicted output for the i^{th} data point, respectively.

2.1.5 Integrated model

In the middle layer, the identified component models are integrated to establish a system model through continuity constraints between the various components, e.g., the compressor discharge enthalpy is equal to the condenser inlet refrigerant enthalpy. The EXV model is not involved in the steady-state model integration; instead, an equality constraint is imposed to enforce the predicted superheat to match the measured value. The model integration stage only involves the identification of the total refrigerant charge and a simple line search is implemented to find the optimal parameter value.

2.2 Dynamic model identification

The system dynamic model is an extension of the steady-state model established in the bottom and middle layers, by incorporating governing differential equations for dynamic variations of the tube wall temperatures of the evaporator and condenser and refrigerant thermal properties. The only tunable parameter of the dynamic model is the tube wall thermal capacitance that characterizes the thermal inertial of the heat exchangers. Since the inherent dynamics of compressor and EXV evolve on much faster time scales than those of the heat exchangers, their steady-state models described in the previous section directly carry over to the dynamic system model. Mass balance is always preserved in the governing differential equations, to be introduced next. Therefore, the initial state variables need to be identified through trial and error so that the system refrigerant charge matches that estimated in the steady-state model (middle layer).

The evaporator dynamic model extends the steady-state one by explicitly considering the conservation differential equations for the refrigerant energy, mass and tube wall energy of the j^{th} control volume given in Equation (12) to Equation (14).

$$\dot{U}_j = m_{j-1}h_{j-1} - m_j h_j + \alpha_{r,j}A_{i,j}\left(T_{w,j} - T_{r,j}\right) \tag{12}$$

$$m_{e,j} = m_{j-1} - m_j \tag{13}$$

$$\dot{E}_j = \left(C_{th,w}\right)_j \dot{T}_{w,j} = \alpha_{a,j}A_{o,j}\left(T_{a,j} - T_{w,j}\right) - \alpha_{r,j}A_{i,j}\left(T_{w,j} - T_{r,j}\right) \tag{14}$$

where U_j is the refrigerant internal energy. $m_{j\text{-}1}$ and m_j represent the inlet and outlet mass flow rates of refrigerant, respectively. $m_{e,j}$ is the time derivative of refrigerant mass held in the jth control volume. E_j is the tube wall energy. $C_{th,w}$ denotes the thermal capacitance of the heat exchanger tube wall for the corresponding control volume, which is estimated in the training process. The HTCs and areas assume the values identified in the bottom and middle layers.

Since the airflow involves very low thermal inertia, a quasi-steady-state energy conservation equation is used

$$C_{p,a}m_a\left(T_{a,j+1} - T_{a,j}\right) = \alpha_{a,j}A_{o,j}\left(T_{a,j} - T_{w,j}\right) \tag{15}$$

The conservation equations from (12) to (15) can be established for all the control volumes of the heat exchanger. Based on the relationship between the refrigerant internal energy and enthalpy

$$u = h - \frac{P}{\rho} \tag{16}$$

where u is the refrigerant specific internal energy and ρ is the refrigerant density, the time derivative of the refrigerant internal energy $\dot{U}_j$ in Equation (12) can be decomposed into terms of time derivatives of the pressure and enthalpy using the chain rule:

$$\dot{U}_j = V_j \left[\left(\left. \frac{\partial \rho_j}{\partial P_e} \right|_{h_j} \right) \dot{P}_e + \left(\left. \frac{\partial \rho_j}{\partial h_j} \right|_{P_e} \right) \dot{h}_j \right] h_j - V_j \dot{P}_e + V_j \rho_j \dot{h}_j \tag{17}$$

where V_j represents the tube internal volume for the j^{th} control volume and the evaporating pressure P_e is assumed to be identical across all control volumes (no pressure drops). Similarly, the mass balance equation of (13) can be re-written as

$$m_{e,j} = V_j \dot{\rho}_j = V_j \left[\left(\left. \frac{\partial \rho_j}{\partial P_e} \right|_{h_j} \right) \dot{P}_e + \left(\left. \frac{\partial \rho_j}{\partial h_j} \right|_{P_e} \right) \dot{h}_j \right] \tag{18}$$

It may be noted that Equations (17) to (18) allows the reformulation of the governing equations using the evaporation pressure and enthalpy as the state variables. The resultant state-space governing equations are

$$\mathbf{Z} \begin{bmatrix} \dot{P}_e \\ \dot{h}_1 \\ \vdots \\ \dot{h}_N \\ \dot{T}_{w,1} \\ \vdots \\ \dot{T}_{w,N} \end{bmatrix} = \begin{bmatrix} m_{in}\left(h_{in} - h_1\right) + \alpha_{r,1} A_{i,1}\left(T_{w,1} - T_{r,1}\right) \\ \vdots \\ m_{in}\left(h_{N-1} - h_{out}\right) + \alpha_{r,N} A_{i,N}\left(T_{w,N} - T_{r,N}\right) \\ m_{in} - m_{out} \\ \alpha_{a,1} A_{o,1}\left(T_{a,1} - T_{w,1}\right) - \alpha_{r,1} A_{i,1}\left(T_{w,1} - T_{r,1}\right) \\ \vdots \\ \alpha_{a,N} A_{o,N}\left(T_{a,N} - T_{w,N}\right) - \alpha_{r,N} A_{i,N}\left(T_{w,N} - T_{r,N}\right) \end{bmatrix} \tag{19}$$

where **Z** is the transformation matrix that is dependent on the evaporation pressure and refrigerant enthalpy of each control volume. The detailed structure of the matrix can be found in Gupta (2007). N denotes the total number of control volumes. m_{in} and m_{out} are the inlet and outlet refrigerant mass flow rates for the evaporator, respectively. Solving the nonlinear differential equation (19) requires inversion of the transformation matrix, the size of which depends on the number of dynamic states ($2N$+1) and the computational complexity of which increases cubically with N, i.e., $O(N^3)$. In the case study, to seek a trade-off between the model's prediction accuracy and computational efficiency, the evaporator was divided into 20 control volumes, i.e., N=20. The differential equations were solved numerically using the fourth-order Runge-Kutta solver with a fixed time step of 0.05 s.

The governing equations for the condenser dynamics share exactly the same form, although a different tube wall thermal capacitance is to be identified through training. The steady-state model parameters in Equation (19), such as the refrigerant- and air-side HTCs, assume values obtained in the bottom and layers as described in Section 2.1. For identification of the dynamic system model, thermal capacitances of the heat exchanger tube walls are estimated so that the predicted superheat matches the experimental data with the minimum RMSRE, considering that the superheat stability is a key requirement for controller design of variable-speed VCS. It should be noted that the thermal capacitance is closely related to the thermal mass of a VCS which enables it to store heat, providing 'inertia' against temperature fluctuations. The thermal capacitance is regarded as one of the most important parameters for system dynamics and control stability.

3. Experimental setup

Figure 3 shows the test variable-speed DX system with a rated cooling capacity of 3 tons, which was used to validate the effectiveness of proposed modeling approach. The unit is a split system. The outdoor unit houses a variable-speed scroll compressor, a condenser coil and a condenser fan, while the indoor unit packages an A-shaped evaporator coil, an ECM-driven supply fan and an EXV. The gas and liquid lines connecting the indoor and outdoor units are both approximately 20' long.

The indoor unit is connected to an indoor environment test loop, which can accommodate flexible load testing with control accuracies of ±0.2 °C for dry bulb temperature and ±0.5% for relative humidity. The outdoor unit, on the other hand, is located in a psychrometric chamber that can reproduce a wide range of outdoor environmental conditions with identical control accuracies to those of the indoor test loop.

Figure 4 shows a schematic diagram of the DX testing platform. The test unit consists of a single vapor compression circuit with R410A as the working fluid. Sensors have been installed to measure key operation variables such as pressures, temperatures, etc. In Figure 4, letters 'T' and 'P' represent the temperature measurement via thermocouples and pressure transducers, respectively. Additional sensors that are not shown in Figure 4, include power meters for the compressor, indoor and outdoor fans, as well as the refrigerant mass flow meter and relative humidity sensors.

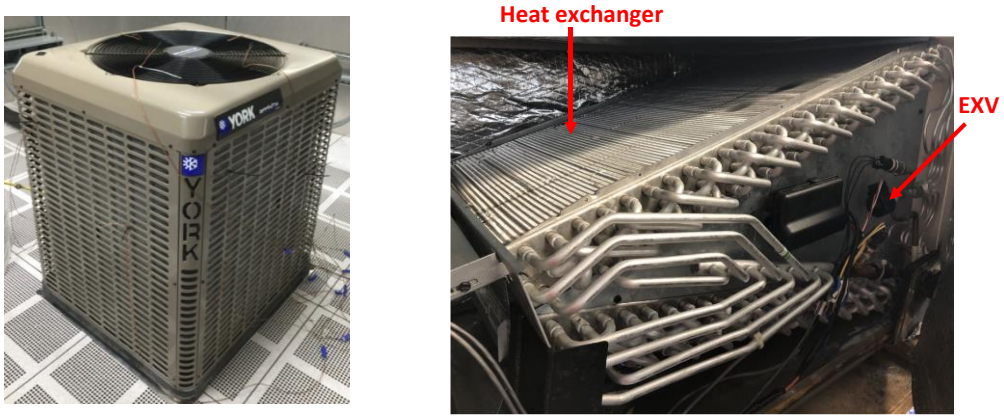

(a) (b)

Figure 3: Variable speed DX system (a) Outdoor unit, (b) Indoor unit

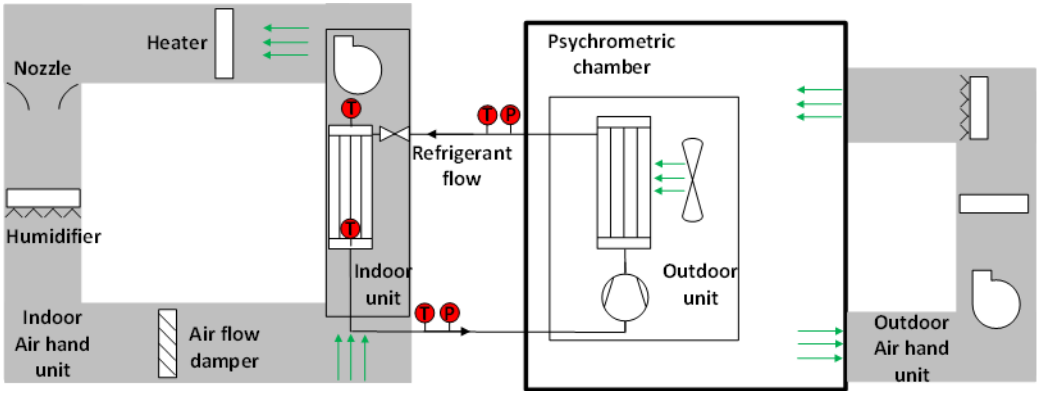

Figure 4: Test rig and sensing instrumentations

4. Test results

The bottom-layer component model identification results are depicted in Figure 5, where different markers are used to distinguish the training and validation points. 56 steady-state data points were collected in the laboratory covering a range of operating and control conditions. Out of the 56 steady-state tests, 46 points were used to train the models and 10 points were utilized for model validation. For the evaporator and condenser models, the heat transfer rate was used as the regression variable and very high accuracy was achieved, with validation RMSRE (VRMSRE) lower than 1.54%. Inconsistent behaviors of the OEM EXV were observed during the experiments with flow characteristics drifting over time. This resulted in reduced accuracy of the EXV model, which was still able to predict the refrigerant mass flow rate with a VRMSRE of less than 7%. The compressor model had a VRMSRE of 3.5%, which is larger than those of the heat exchangers; this is because the power prediction relies on the sub-models for mass flow, combined isentropic efficiency and heat loss and the corresponding sub-model inaccuracies added up to the total error of 3.5%. The modeling details can be found in Liu and Cai (2021). The results prove that the steady-state training

methodology (bottom and middle layers) can accurately capture the system steady-state behaviors and provide reliable heat transfer parameters such as HTC to be used in the dynamic model.

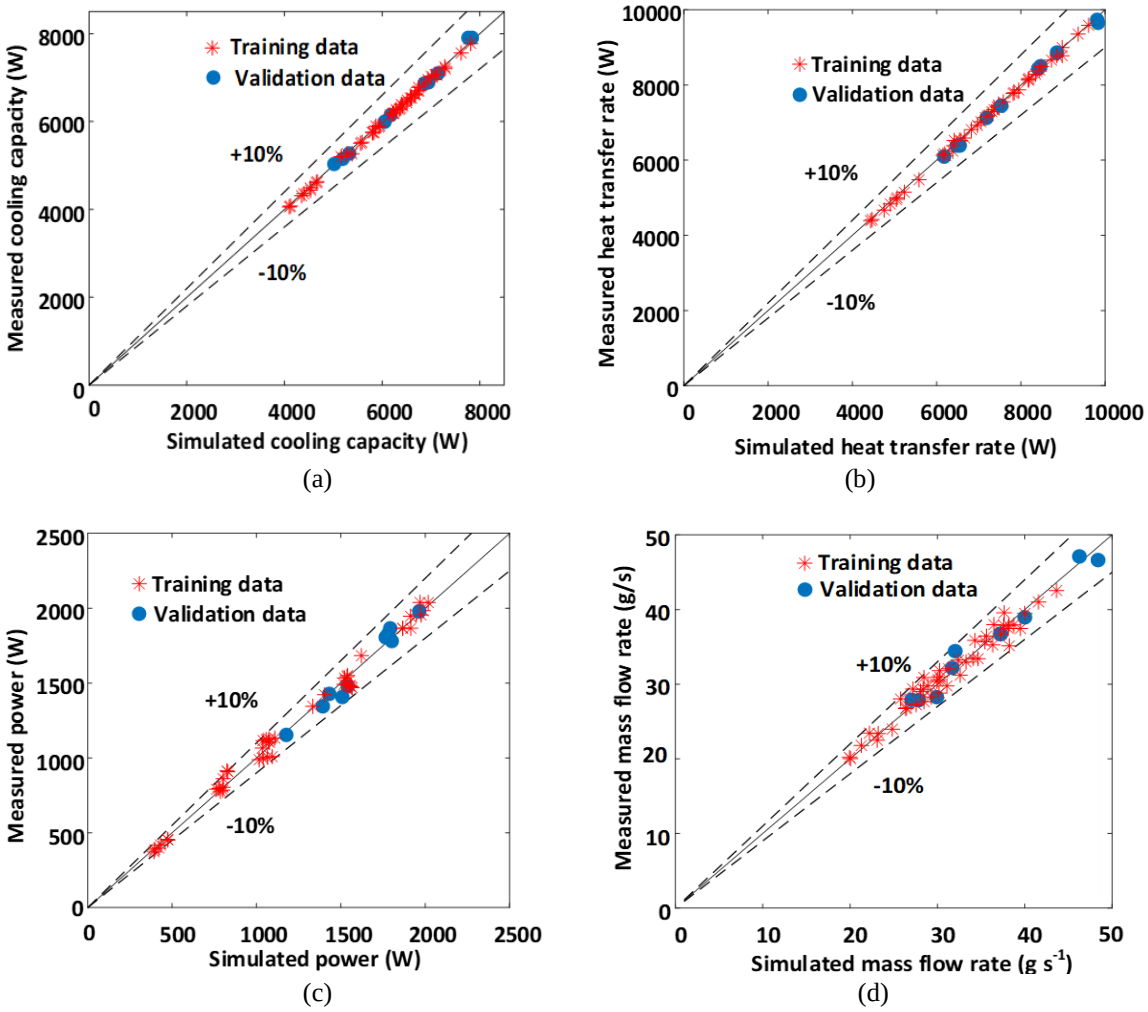

Figure 5: Comparisons of component model predictions and experimental results
(a) Evaporator, cooling capacity, VRMSRE=1.54%, (b) Condenser, heat transfer rate, VRMSRE=0.93%, (c) Compressor, power consumption, VRMSRE=3.49%, (d) EXV, mass flow rate, VRMSRE=6.95%.

The top layer training only involves two estimation parameters, i.e., the tube wall thermal capacitances for the evaporator and condenser, and the superheat temperature is used as the regression output. The comparisons between the predicted superheat with different values of $C_{th,w}$ and the measured superheat are shown in Figure 6, where '$C_{th,r}$' denotes the reference evaporator tube wall thermal capacitance calculated from detailed coil geometries provided by the manufacturer. Simulation results of different capacitance values are depicted in Figure 6. The estimated thermal capacitance was 40% higher than the reference capacitance estimated from the spec sheet, possibly because the estimated capacitance also captured the inertia of the superheat sensor (thermocouple installed in the suction line with grounded shell). The estimated thermal capacitance led to transient behaviors best matching the measurements. Small thermal capacitance ($0.5C_{th,r}$) led to a lower system thermal inertia and fast response, while a large thermal capacitance ($2C_{th,r}$) resulted in slow responses.

The boundary conditions of a validation test are shown in Figure 7, where 'CFM' represents the supply air flow rate delivered by the indoor unit, and 'CAI' and 'EAI' stand for the condenser/evaporator air inlet temperatures, respectively. In the test, step changes were imposed for the compressor speed, indoor CFM, EXV opening, and evaporator and condenser air inlet temperatures to evaluate the system transient responses. The comparisons of the measured and predicted cooling capacity, power consumption, evaporator/condenser saturation temperatures and

superheat temperature are depicted in Figure 8. The results demonstrated that the identified dynamic model could accurately capture the system dynamics. For this specific validation test, the model prediction RMSREs are 1.1% for the cooling capacity, 4.4% for compressor power consumption, less than 0.8˚K for the saturated evaporation/condensation temperatures and 1.3˚K for the superheat temperature.

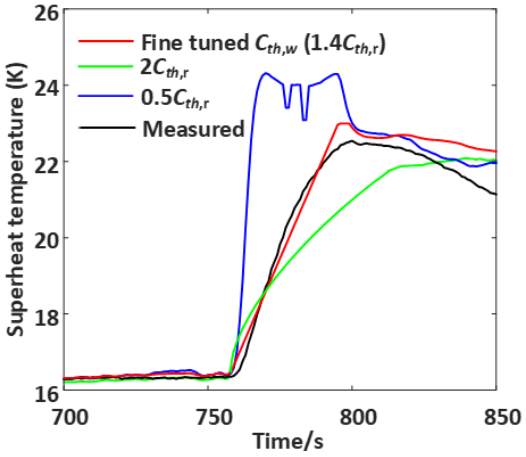

Figure 6: Comparisons of superheat at different thermal capacitance

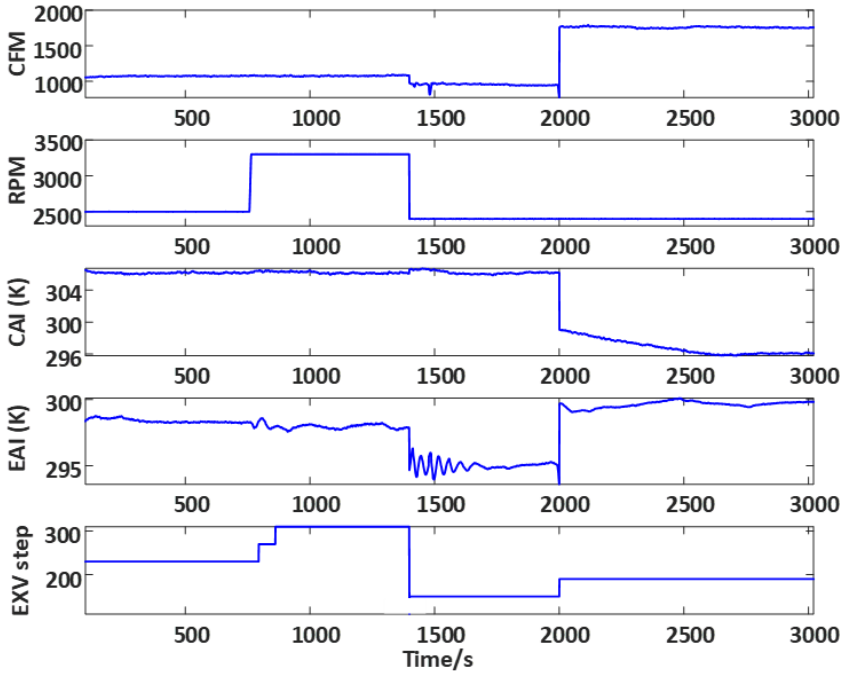

Figure 7: Boundary conditions of experimental validation

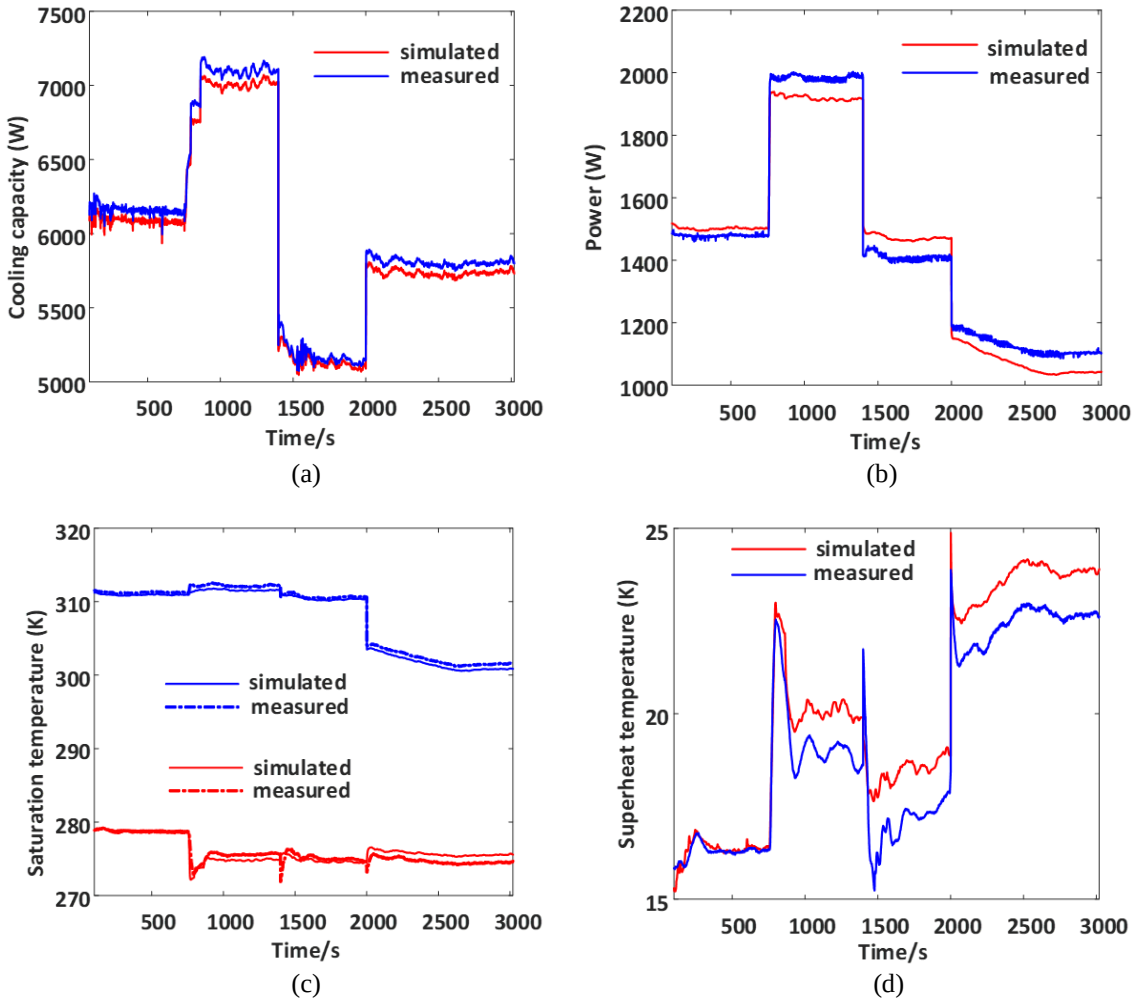

Figure 8: Comparisons of system dynamic performance between simulation and experiment (a) Cooling capacity, RMSRE=1.14%, (b) Power consumption, RMSRE=4.39%, (c) Saturation temperature, for T_e, RMSE=0.81 ˚K; for T_c, RMSE=0.68 ˚K, (d) Superheat temperature, RMSE=1.27 ˚K.

5. Conclusions

A multi-layer training methodology for gray-box dynamic modeling of variable-speed vapor compression systems is presented in this paper. The overall methodology decomposes the model estimation task into multiple layers, that can be implemented in parallel or in series, and consequently improves the model estimation efficiency and reliability. Employing a finite control volume approach for characterizing the thermal behaviors of heat exchangers, the proposed methodology has advantages including low training data requirement, high computational efficiency and superb model accuracy. To demonstrate the efficacy, the methodology was applied to modeling of a 3-ton variable-speed heat pump. The experimental validation verified that the established model can provide accurate predictions of both steady-state and dynamic behaviors under a range of operation conditions. The developed model will be used to facilitate optimized control algorithm design for variable-speed vapor compression systems and to evaluate the potentials for provision of fast ancillary services to the electric grid.

REFERENCES

Admiraal, D. M., & Bullard, C. W. (1993). Heat transfer in refrigerator condensers and evaporators. *Air Conditioning and Refrigeration Center*. College of Engineering. University of Illinois at Urbana-Champaign.

Beghi, A., & Cecchinato, L. (2009). A simulation environment for dry-expansion evaporators with application to the design of autotuning control algorithms for electronic expansion valves. *Int. J. Refrig.*, 32(7), 1765-1775.

Belman, J. M., Navarro-Esbrí, J., Ginestar, D., & Milian, V. (2010). Steady-state model of a variable speed vapor compression system using R134a as working fluid. *Int. J. Energy Res*., 34(11), 933-945.

Bendapudi, S., & Braun, J. E. (2002). Development and validation of a mechanistic, dynamic model for a vapor compression centrifugal liquid chiller. *Report of ASHRAE*.

Bergman, T. L., Incropera, F. P., DeWitt, D. P., & Lavine, A. S. (2011). *Fundamentals of heat and mass transfer*. New York: John Wiley & Sons.

Catano, J., Zhang, T., Wen, J. T., Jensen, M. K., & Peles, Y. (2013). Vapor compression refrigeration cycle for electronics cooling–Part I: Dynamic modeling and experimental validation. *Int. J. Heat Mass Transf*., 66, 911-921.

Catano, J., Lizarralde, F., Zhang, T., Wen, J. T., Jensen, M. K., & Peles, Y. (2013). Vapor compression refrigeration cycle for electronics cooling–Part II: gain-scheduling control for critical heat flux avoidance. *Int. J. Heat Mass Transf*., 66, 922-929.

Chen, J. C. (1966). Correlation for boiling heat transfer to saturated fluids in convective flow. *Ind. Eng. Chem. Process. Des. Dev*., 5(3), 322-329.

Chen, W., & Deng, S. (2006). Development of a dynamic model for a DX VAV air conditioning system. *ENERG CONVERS MANAGE*., 47(18-19), 2900-2924.

Chen, Y., Halm, N. P., Groll, E. A., & Braun, J. E. (2000). A Comprehensive Model of Scroll Compressors Part II: Overall Scroll Compressor Modeling.

Davies, A., & TC, D. (1973). SINGLE AND TWO-PHASE FLOW OF DICHLORODIFLUOROMETHANE, (R12), THROUGH SHARP-EDGED ORIFICES.

Electricity Data. 2020. U.S. Energy Information Administration (EIA). https://www.eia.gov/outlooks/aeo/pdf/AEO2020%20Electricity.pdf (accessed Nov 2020)

Gupta, A. (2007). Reduced order modeling of heat exchangers using high order finite control volume models (Master dissertation).

Kapadia, R. G., Jain, S., & Agarwal, R. S. (2009). Transient characteristics of split air-conditioning systems using R-22 and R-410A as refrigerants. *HVAC&R RES*., 15(3), 617-649.

Li, B., & Alleyne, A. G. (2010). A dynamic model of a vapor compression cycle with shut-down and start-up operations. *Int. J. Refrig*., 33(3), 538-552.

Li, W. (2013). Simplified modeling analysis of mass flow characteristics in electronic expansion valve. *Appl. Therm. Eng*., 53(1), 8-12.

Liu, H., & Cai, J. (2021). A robust gray-box modeling methodology for variable-speed direct-expansion systems with limited training data. *Int. J. Refrig.*, (under review).

Navarro-Esbrí, J., Ginestar, D., Belman, J. M., Milián, V., & Verdú, G. (2010). Application of a lumped model for predicting energy performance of a variable-speed vapour compression system. *Appl. Therm. Eng*., 30(4), 286-294.

Rasmussen, B. P. (2012). Dynamic modeling for vapor compression systems—Part I: Literature review. *HVAC&R RES*., 18(5), 934-955.

Reindl, D. I. J. D. T., & Klein, P. S. A. (2000). A semi-empirical method for representing domestic refrigerator/freezer compressor calorimeter test data.

Shah, M. M. (1979). A general correlation for heat transfer during film condensation inside pipes. *Int. J. Heat Mass Transf*., 22(4), 547-556.

Tandon, T. N., Varma, H. K., & Gupta, C. P. (1985). A void fraction model for annular two-phase flow. *Int. J. Heat Mass Transf*., 28(1), 191-198.

Wang, C. C., Fu, W. L., & Chang, C. T. (1997). Heat transfer and friction characteristics of typical wavy fin-and-tube heat exchangers. *Exp. Therm. Fluid Sci*., 14(2), 174-186.

Winandy, E., Saavedra, C., & Lebrun, J. (2002). Experimental analysis and simplified modelling of a hermetic scroll refrigeration compressor. *Appl. Therm. Eng*., 22(2), 107-120.